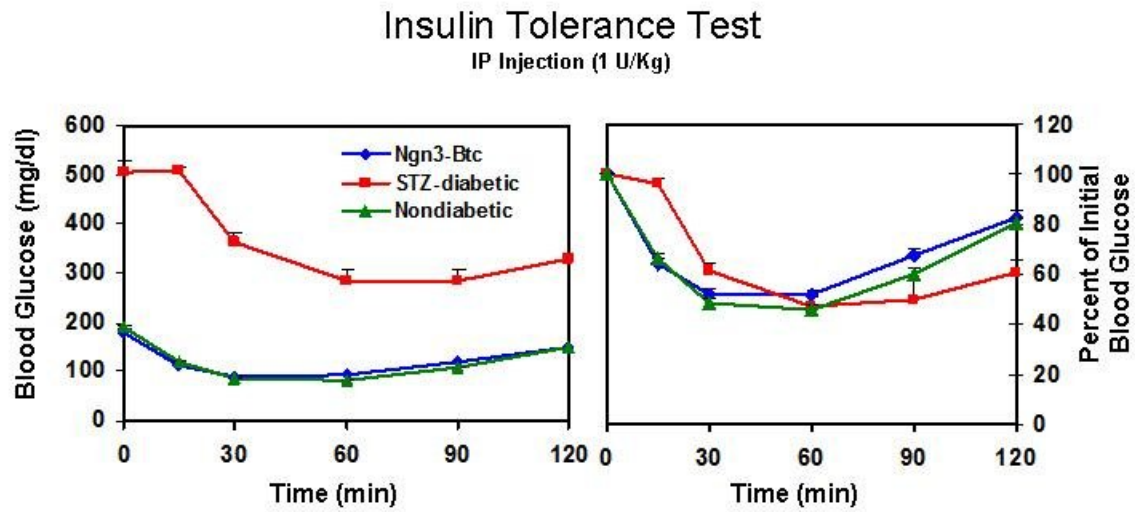


## Supplemental Fig. 1



## **Supplemental Text**

### **Supplemental Methods**

**Animals:** Diabetes was induced by injecting C57Bl6/J mice (from Jackson Labs, Bar Harbor, ME, housed in a pathogen free vivarium in a 12 hour light-dark cycle with ad-lib chow and water) intra-peritoneally (IP) with streptozotocin (STZ, Sigma) 125 mg/kg on two consecutive days. Diabetic mice were monitored regularly with body weights and 4 hour fasting blood glucoses determined by tail snip and using a One Touch glucometer. Diabetes was defined as two consecutive blood glucoses  $\geq 250$  mg/dl. HDAd were injected intravenously via tail vein 2 weeks after STZ. A glucose tolerance test was performed, 6 weeks after treatment, on mice that were fasted 4 hours and injected with 1.5 gm/kg of D-Glucose IP, and blood collected at 0, 15, 30, 60, 120 min for assaying glucose and insulin. An Insulin tolerance test was performed by injecting 1U/Kg of insulin IP and measuring blood glucose at 0, 15, 30, 60 and 90 minutes after injection. Mice were anesthetized and tissues were collected at stated time points and processed for RNA, protein, insulin content, immunohistochemistry and immunofluorescence microscopy as described below. BrdU (15 $\mu$ l/gm) (GE Healthcare) was injected 2 hours prior to sacrifice for measuring cellular proliferation.

**Helper-Dependant Adenoviral Vectors:** Mouse Ngn3 cDNA (a gift from Dr. Ming-Jer Tsai) and mouse Btc cDNA were cloned into a pBluescript II KS vector (Stratagene, La Jolla, California). The fully sequenced cDNAs were then sub-cloned into pLPBL1 shuttle plasmid with an elongation factor 1 $\alpha$  (BOS) promoter and rabbit  $\beta$ -globin polyadenylation signal. We used p-delta28 plasmids as backbone for the HDAd and these were amplified as described previously (Ng et al., 1999). Diabetic mice with stable hyperglycemia for at least a week were administered a single IV injection of HDAd vectors via tail vein. To exclude any non-specific effect related to vector dose, the total vector dose was maintained at  $6 \times 10^{11}$  vp in all treatment groups: ( $5 \times 10^{11}$  vp Ngn3 +  $1 \times 10^{11}$  vp Btc), ( $5 \times 10^{11}$  vp Ngn3 +  $1 \times 10^{11}$  vp empty vector), ( $1 \times 10^{11}$  vp Btc +  $5 \times 10^{11}$  vp empty vector) and ( $6 \times 10^{11}$  vp empty vector).

**Quantitative Real-time PCR for Gene Expression Analysis:** Liver and pancreas were removed at stated time points from anesthetized mice, snap frozen in liquid nitrogen and stored at -80C. They were homogenized in Trizol Reagent (Invitrogen, CA) and total RNA extracted as per manufacturer's instructions. This RNA was then subjected to an on-column purification and DNaseI digestion (RNeasy mini, Qiagen) to remove any genomic DNA contamination. The eluted RNA was quantitated and stored at -80C. RT was performed by using 20 $\mu$ g of RNA with Superscript RT III cDNA synthesis kit (Invitrogen, CA). We performed quantitative real-time PCR using SYBR Green reagent (BioRad). The Ct values were obtained after normalizing to the non-reactive ROX dye which served as a reference control. Using the delta-delta-Ct method, after normalizing to house keeping genes (eEIF-1 $\gamma$  & GAPDH), we quantified various transcripts using appropriate primers (Supplemental Table 2) and analyzed melting curves to confirm accurate readings.

**Insulin and C-Peptide Content:** Liver was homogenized in 70% ethanol and 0.2 N HCl and extracted overnight at 4°C. The samples were spun down and an aliquot of the supernatant was used for analysis after neutralization with 0.4M Tris (pH 8.0) to bring the sample pH to 7.3. This was used to measure insulin using the ultra sensitive mouse insulin assay kit (Merckodia) or the C-peptide ELISA kit (Wako) and normalized to the protein content measured by the modified Lowry assay (Dc Reagent, BioRad) or to the tissue weights and total body weight measured at the time of sacrifice.

**In situ Liver Perfusion:** We anesthetized mice with Avertin and cannulated their portal vein for infusion under direct visualization using a dissecting microscope. The portal vein was ligated below the cannulation to prevent any blood leaking into the perfusion circuit. The inferior vena cava (IVC) was ligated above the renal veins and the aorta transected above the diaphragm. A catheter was placed in the IVC via the right atrium with the tip at the entry of the hepatic veins to collect the effusate. After initial washout, we perfused the isolated liver with KRB buffer (119mM NaCl, 4.7mM KCl, 25 mM NaHCO<sub>3</sub>, 2.5mM CaCl<sub>2</sub>, 1.2mM MgSO<sub>4</sub>, 1.2mM KH<sub>2</sub>PO<sub>4</sub> and 0.25%BSA) containing different concentrations of glucose in a step-up pattern at 1.2 ml/min using a peristaltic pump. Finally, we added glibenclamide at a concentration of 10 nM after a washout. All effusate was collected on ice and then frozen at -20°C until assayed for insulin.

**In Vitro GSIS:** Livers from Ngn3-Btc-treated diabetic mip-GFP mice or nondiabetic control mice were collagenase IV (Sigma) digested by perfusion through the portal vein, a single cell suspension obtained after filtration through a 100 micron mesh and subjected to FACS using propidium iodide to exclude non-viable cells and GFP to sort cells. Both GFP negative and positive cells were collected from treated mice (only GFP negative cells were detected from nondiabetic mice) which were collected. The cells were plated onto 24 well plates overnight. An insulin secretion study was performed as described (Kojima et al., 2003).

**Immunofluorescence Microscopy and Immunohistochemistry:** We fixed liver and pancreas in 10% formalin overnight or perfusion fixed them with formaldehyde/gluteraldehyde solution and then processed tissues into 5mm paraffin embedded sections. These were deparaffinised and hydrated using standard protocols with graded ethanol solutions. Antigen retrieval was performed using proteinase K or heating in 0.1M sodium citrate buffer (pH 6.0) and all primary antibody incubations were done overnight at 4°C and the secondary antibody incubations were done at room temperature for 1 h. The secondary antibodies were fluorophore conjugated for visualization and the slides were mounted with DAPI in the mounting medium for immunofluorescence. For immunohistochemistry, a biotin labeled secondary antibody was used and the Elite ABC kit and Novared substrate (Vector labs) kit was used for visualization. Primary Antibodies used were insulin (1:100 guinea pig polyclonal, Abcam), proinsulin (1:500 guinea pig polyclonal, Progen biotechnik), Glucagon (1:75 rabbit anti-human, Dako), pancreatic polypeptide (1:200 rabbit anti-human, Dako), somatostatin (1:200 rabbit anti-human, Dako), albumin (1:100 rabbit polyclonal, Abcam), CK19 (1:200 mouse anti-human, MP Biomedicals), A6 (1:200 rat anti-mouse, gift from Dr. Valentina M. Factor, NIH), BrdU (1:200 rat anti-BrdU, Abcam), PCNA (1:500

mouse monoclonal, Santa Cruz Biotechnology), GFP (1:500 AlexaFluor 488 conjugated rabbit anti-GFP, Invitrogen), Thy1 (1:200 mouse monoclonal, Santa Cruz Biotechnologies), elastase (1:200 rabbit polyclonal, Abcam), Pdx1 (1:5000 goat anti-mouse, gift from Dr. Christopher Wright), Ngn3 (1:2000, Beta Cell Biology Consortium, Univ. of Pennsylvania), betacellulin (1:200, Cell Sciences) and Nkx6.1 (1:100, Beta Cell Biology Consortium, Univ. of Pennsylvania). The immunohistochemistry for Pdx1, Ngn3, Nkx6.1 and Btc are shown in Supplemental Figures 16-18. Secondary antibodies (Alexa Fluor 488: Goat anti-guinea pig; Alexa Fluor 546: Goat anti-rabbit, Goat anti-rat; Alexa Fluor 533: Donkey anti-mouse; Alexa Fluor 647: Chicken anti-mouse, Goat anti-rat – all from Invitrogen at a dilution of 1:500) were used as indicated. Immunofluorescence microscopy was performed using an Axiovert (Zeiss) microscope with Axiovision imaging software 4.0. All the images within the same experiment were acquired at the same settings and processed identically. In all images, the AlexaFluor 647 is pseudo-colored magenta. We used a laser scanning confocal microscope (Zeiss LSM 510 META Confocal/Spectral Imaging Microscope) for albumin and insulin co-localization (Supplemental Figure 11).

**Bone marrow transfer experiments indicate that periportal islet like clusters are not derived from bone marrow-derived cells:** Bone marrow was obtained from the femur of donor mice (male mip-GFP transgenic mice) and washed twice with HBSS after filtration through a 70  $\mu\text{m}$  mesh. Hypotonic RBC lysis was performed for 17 seconds using distilled water and the mononuclear cells were counted. Two million mononuclear cells were transfused via the tail vein into lethally irradiated recipient mice (female Rosa26-lacZ mice) that were  $\gamma$ -irradiated with 9cG divided into 2 doses separated by 4 hours. The marrow was transfused within 1 hour after the second irradiation. Diabetes was induced in the recipients; we then treated them with either Ngn3-Btc or with empty vector. We analyzed for insulin positive cells in the liver of the mice treated with Ngn3-Btc for  $\beta$ -gal (recipient) or eGFP (donor derived) expression. We found that all periportal insulin-producing cells to be  $\beta$ -gal positive with none being eGFP positive, indicating that they are not derived from the donor bone marrow (Supplemental Figure. 9).

**Lineage Tracing:** Transgenic mice (Rosa26 Stop-Lox-eGFP reporter and Albumin-Cre mice) were purchased from Jackson Labs. The ROSA26 promoter driven ubiquitous eGFP expression is blocked by the presence of an intervening STOP sequence flanked by loxP sites. When crossed with transgenic mice carrying the albumin promoter-driven Cre recombinase gene, the Cre removes the loxP-flanked STOP sequence during early development in the liver, turning on eGFP expression in all progeny cells, driven by the ROSA26 promoter. In cells that never expressed albumin, the Cre recombinase is not expressed and the STOP sequence remains and prevents the expression of eGFP. We generated these ROSA26 Stop-Lox-eGFP x Albumin-Cre mice and induced diabetes in them as described above. These diabetic mice were then treated with HDAd-Ngn3-Btc or with Empty vector as described. The mice were then sacrificed and the liver was removed and processed for immunostaining to look for co-localization of insulin, GFP and albumin.

**Laser Capture Microdissection (LCM) and Global Gene Expression Profiling:** Liver and pancreas were embedded in OCT compound and frozen on dry ice and stored at -80°C. These were cryosectioned (7µm) and nuclear-stained (Histogene staining kit, Molecular devices) in a RNase free environment. LCM was performed using the Veritas microdissection system (Molecular devices). Cells with a high nuclear-cytoplasmic ratios present in clusters in the periportal region and large parenchymal hepatocytes were isolated and collected from each group separately. Total RNA was extracted using the Pico Pure RNA isolation kits (Molecular Devices) and amplified twice with the RiboAmp kits (Molecular Devices). This was DNaseI treated, quantitated, reverse transcribed and used in PCR reactions to assess gene expression. For PCR of LCM amplified RNA, primers were designed that were in the 3' end of the coding sequence. All PCR reactions were performed for 40 cycles except for Ins1, Ins2, Albumin and β-actin which were performed for 32 cycles. Electrophoreses was performed on the PCR products on a 1.2% agarose gel. In separate experiments, GFP positive cells were collected by LCM from the Ngn3-Btc treated diabetic mip-GFP mice and also from the liver and islets of nondiabetic mip-GFP mice. Oval cells were collected by LCM from the livers of mice that were put on a 1/2CD+E {choline deficient diet mixed with regular chow 1:1 ratio and with DL-ethionine (Sigma) 0.15% supplemented via drinking water, (Akhurst et al., 2001)} diet for 3 weeks. 3 mice were used in each group. RNA was extracted, amplified, DNase I digested and 20 µg reverse transcribed as described above. All the samples were labeled with Cy5 dye (Turbo labeling kit, Molecular Devices) while a pool from equal quantities of the 3 samples of normal islet RNA was labeled with Cy3 dye which served as the reference sample. Equal quantities of Cy5 sample and Cy3 reference samples were mixed together and hybridized as per the manufacturers protocol to 11 (3 each of neo-islets, pancreatic islets, chemically-induced oval cells and 2 of normal hepatocytes) PancChip6.1 cDNA microarrays (Beta Cell Biology Consortium, Univ. of Pennsylvania), scanned on an Agilent scanner, the images analyzed (Genepix pro 6.1) and the Cy5/Cy3 ratios log<sub>2</sub> transformed using median intensities, normalized by the lowess normalization and standard deviation regularization {MIDAS software, (Saeed et al., 2003)}. This data was transferred to MeV software (Saeed et al., 2003) and a higher-order analysis using ANOVA testing for 4 groups for 0.01 significance was performed and the resulting data was then subjected to a correspondence analysis.

## Reference List

- Akhurst,B., Croager,E.J., Farley-Roche,C.A., Ong,J.K., Dumble,M.L., Knight,B., and Yeoh,G.C. (2001). A modified choline-deficient, ethionine-supplemented diet protocol effectively induces oval cells in mouse liver. *Hepatology* 34, 519-522.
- Kojima,H., Fujimiya,M., Matsumura,K., Younan,P., Imaeda,H., Maeda,M., and Chan,L. (2003). NeuroD-beta-cellulin gene therapy induces islet neogenesis in the liver and reverses diabetes in mice. *Nat. Med.* 9, 596-603.
- Ng,P., Parks,R.J., Cummings,D.T., Eveleigh,C.M., Sankar,U., and Graham,F.L. (1999). A high-efficiency Cre/loxP-based system for construction of adenoviral vectors. *Hum. Gene Ther.* 10, 2667-2672.
- Saeed,A.I., Sharov,V., White,J., Li,J., Liang,W., Bhagabati,N., Braisted,J., Klapa,M., Currier,T., Thiagarajan,M., Sturn,A., Snuffin,M., Rezantsev,A., Popov,D., Ryltsov,A., Kostukovich,E., Borisovsky,I., Liu,Z., Vinsavich,A., Trush,V., and Quackenbush,J. (2003). TM4: a free, open-source system for microarray data management and analysis. *Biotechniques* 34, 374-378.



### **Supplemental Figure Legends**

**Supplemental Figure 1:** Insulin tolerance test (with an IP injection of 1U/Kg of Insulin) in Ngn3-Btc-treated diabetic mice compared to untreated STZ-diabetic and nondiabetic control mice (n=3-4). Left panel shows the absolute blood glucose values and the right panel shows the percentage drop after insulin injection. All values are mean±SEM.

**Supplemental Figure 2:** (A) Blood glucose during a 72 h fast in Ngn3-Btc-treated and empty vector-treated nondiabetic mice. All values are mean±SEM. (B-E) Representative IF liver and pancreas sections from the Ngn3-Btc-treated and empty vector-treated nondiabetic mice. The arrow in (B) points to a periportal insulin positive cluster in the Ngn3-Btc-treated mouse liver. The pancreatic sections show normal islets with both treatment groups. Scale bar represents 20µm. PV, Portal vein

**Supplemental Figure 3:** Liver C-peptide content (ng) per mg protein (upper panel), normalized to the whole organ weight (middle panel) and normalized to the body weight (lower panel) (n=3-4) is shown from the Ngn3-Btc treated mouse livers at indicated time points and contrasted to that seen in a nondiabetic control pancreas. \* p≤0.05.

**Supplemental Figure 4:** Liver sections stained by IF for insulin (green), Elastase (pseudo-colored magenta) and DAPI were imaged and the merged image from diabetic mice treated with Ngn3-Btc (A) or empty vector (B); for comparison we also show a pancreas section from a nondiabetic control mouse pancreas (C) showing an insulin staining islet with surrounding exocrine acinar tissue. No elastase expression is seen in the neo-islets in panel A. Scale bar represents 50µm. PV, Portal vein

**Supplemental Figure 5:** RT-qPCR of total liver RNA (n=3-5) from Ngn3-Btc or empty vector-treated mice, 3 weeks after treatment, for PEPCK gene expression normalized to that of nondiabetic control liver PEPCK expression, after all have been normalized to their own housekeeping genes (GAPDH and eEF1γ). \* p≤0.05; ns-not significant

**Supplemental Figure 6:** Representative liver sections stained for insulin (green) from diabetic mice treated with Ngn3-Btc (upper), Ngn3-only (middle) and empty vector (lower). The orange arrows represent insulin-positive cell clusters in the periportal regions in the Ngn3-Btc and Ngn3-only treated mice. No such cell clusters are seen with empty vector treatment. Scale bar represents 100µm. PV, Portal vein

**Supplemental Figure 7:** Representative sections stained for GFP (green) and DAPI and the merged image shown of transgenic mip-GFP diabetic mouse liver treated with Ngn3-Btc (A-C) at different time points or with empty vector (D). The white arrowheads represent GFP-positive and the orange arrowheads show the GFP-negative hepatocytes at the 3 week time point (A). The arrowheads in B and C point to GFP-positive periportal small cell clusters in the Ngn3-Btc treated mice. No GFP-positive cell is seen in the empty vector-treated mouse in D. Scale bar represents 50µm. PV, Portal vein

**Supplemental Figure 8:** Representative sections of empty vector (A-C) and Ngn3-only (D-L) treated STZ-diabetic mouse livers stained for insulin (left panels); pancreatic polypeptide (PP), somatostatin (SS) and glucagon (Gcg), middle panels; or merged images - right panels by IF. Individual hormone-producing cells can be seen for each of the hormones (blue arrows for insulin and orange arrows for others). No primary antibody control is shown (M-O). Scale bar represents 20 $\mu$ m.

**Supplemental Figure 9:** Representative sections of bone marrow transplanted (Donor – mipGFP and Recipient – Rosa-LacZ) diabetic mouse liver treated with Ngn3-Btc stained for insulin (red – A),  $\beta$ -gal (pseudo-colored magenta – B), GFP (green – C) and merged image (purple – D) by immunofluorescence. All the insulin (red) expression co-localizes with the  $\beta$ -gal (magenta) (from the recipient) expression and no GFP (donor bone marrow) expression is seen. PV, Portal vein

**Supplemental Figure 10:** Representative sections of nondiabetic bi-genic (Rosa-Stop-LoxP-eGFP x Alb-Cre) mouse liver (A-F) or from negative control Rosa-Stop-LoxP-eGFP mouse (G-I) stained for GFP (green – panels A, D, G), A6 (red - B, E, H) and merged images (panels - C, F, I) by immunofluorescence. Green staining are cells that express GFP indicating the albumin-expressing lineage, red staining indicates cells that express the oval cell specific antigen A6 while yellow staining in merged images indicates A6 expression in cells of the albumin-expressing lineage. D-F are a higher magnification of the inset area in panels A-C. Scale bar represents 50 $\mu$ m in panels A-C & G-I and 20 $\mu$ m in D-F.

**Supplemental Figure 11:** Representative section of Ngn3-Btc treated STZ-diabetic mouse liver 3 weeks after treatment immunostained with insulin (green - A), albumin (red – B) and the merged images (C), imaged with confocal microscopy, are shown. Yellow indicated co-expression of insulin and albumin. Scale bar represents 20 $\mu$ m.

**Supplemental Figure 12:** Periportal clusters of orange-red staining A6 positive oval cells by immunohistochemistry in Ngn3-only treated diabetic mice (A-B). Scale bar represents 50 $\mu$ m. PV, Portal vein. C-F: Representative IF sections of Ngn3-Btc-treated diabetic mouse liver - immunostained for insulin (green), oval-specific antigen A6 (pseudo-colored magenta), Thy1, which is also expressed by oval cells (red), and the merged images with DAPI (right panel). Scale bar represents 20 $\mu$ m.

**Supplemental Figure 13:** Immunofluorescence staining of a periportal neo-islet in Ngn3-Btc-treated mouse liver with insulin (green - A), oval specific antigen A6 (pseudo-colored magenta – B), CK-19, an oval cell and biliary epithelial antigen, (red - C) and the Merged images with nuclear staining with DAPI (D) are shown. White arrow marks a cell that is positive for insulin, A6 and CK-19, indicating oval cell origin of the insulin-positive cell, while the red arrow points to a cell that is positive only for CK-19, indicative of a biliary cell. Scale bar represents 50 $\mu$ m. PV, Portal vein.

**Supplemental Figure 14:** Immunofluorescence staining of a periportal neo-islet in Ngn3-only-treated mouse liver with insulin (green - A), oval specific antigen A6



(pseudo-colored magenta – B), CK-19, an oval cell and biliary epithelial antigen, (red - C) and the Merged images with nuclear staining with DAPI (D) are shown. White arrow shows cells positive for insulin, A6 and CK-19. Scale bar represents 20 $\mu$ m. PV, Portal vein.

**Supplemental Figure 15:** PCNA staining (upper panels) show significant proliferative activity in the periportal oval cells as compared to the neighboring hepatocytes, more so with Ngn3-Btc (left) than with Ngn3-only (right) treatment. Scale bar represents 50 $\mu$ m. PV, Portal vein.

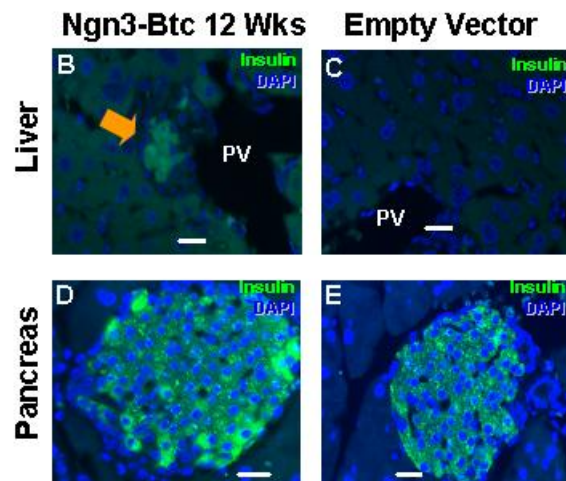
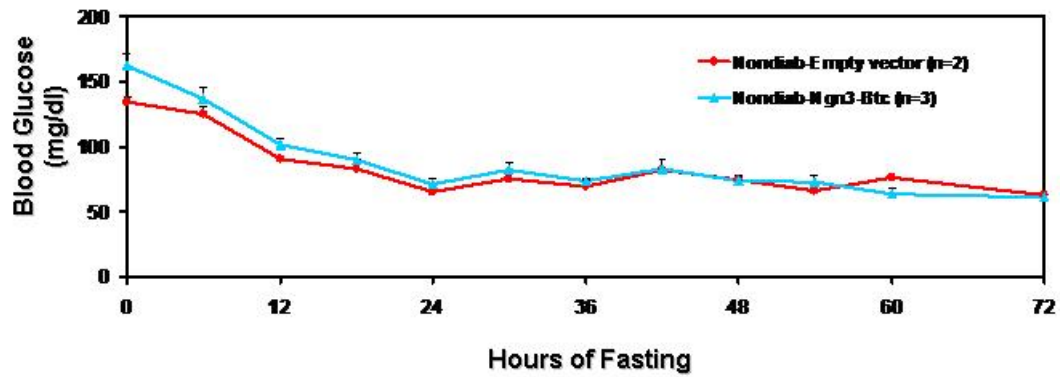
**Supplemental Figure 16-17:** Immunohistochemistry of Ngn3-Btc treated liver shows Pdx1, Ngn3 and Nkx6.1 staining in the periportal cells in contrast to none seen with empty vector treatment. Scale bar represents 20 $\mu$ m. PV, Portal vein.

**Supplemental Figure 18:** Immunohistochemistry of Ngn3-Btc treated liver shows strong staining diffusely in the liver while none is seen with empty vector treatment. Scale bar represents 50 $\mu$ m. PV, Portal vein.

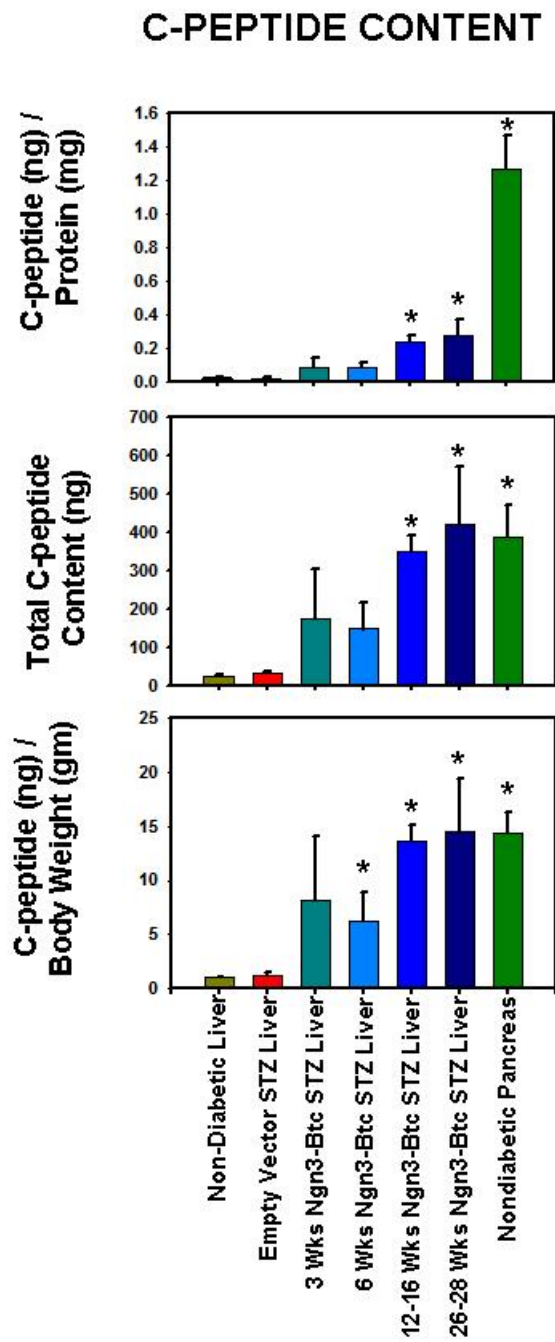
## Supplemental Fig. 2

## Treated Non-Diabetic Mice

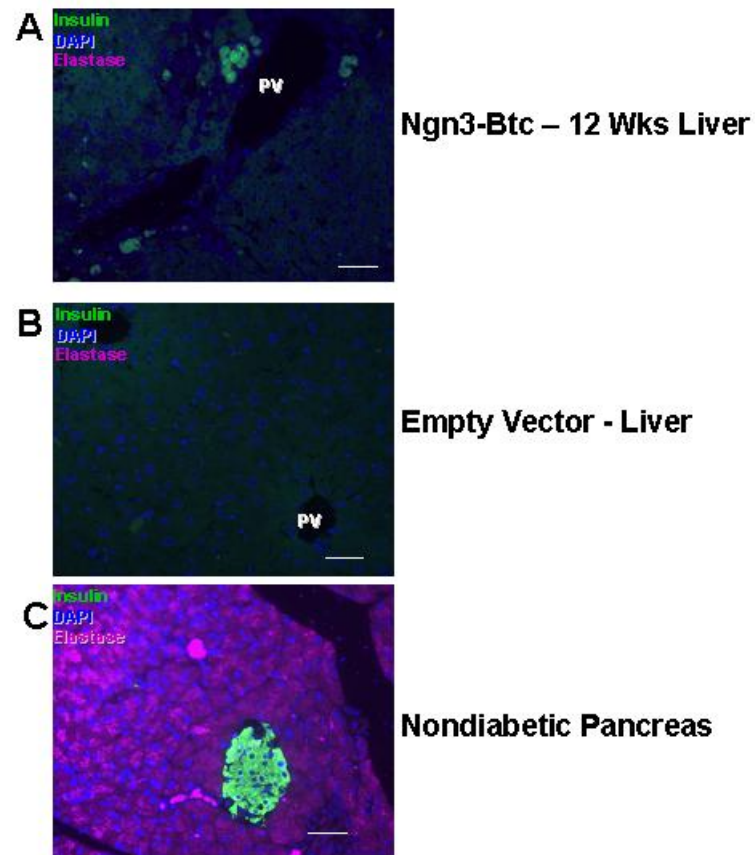
A



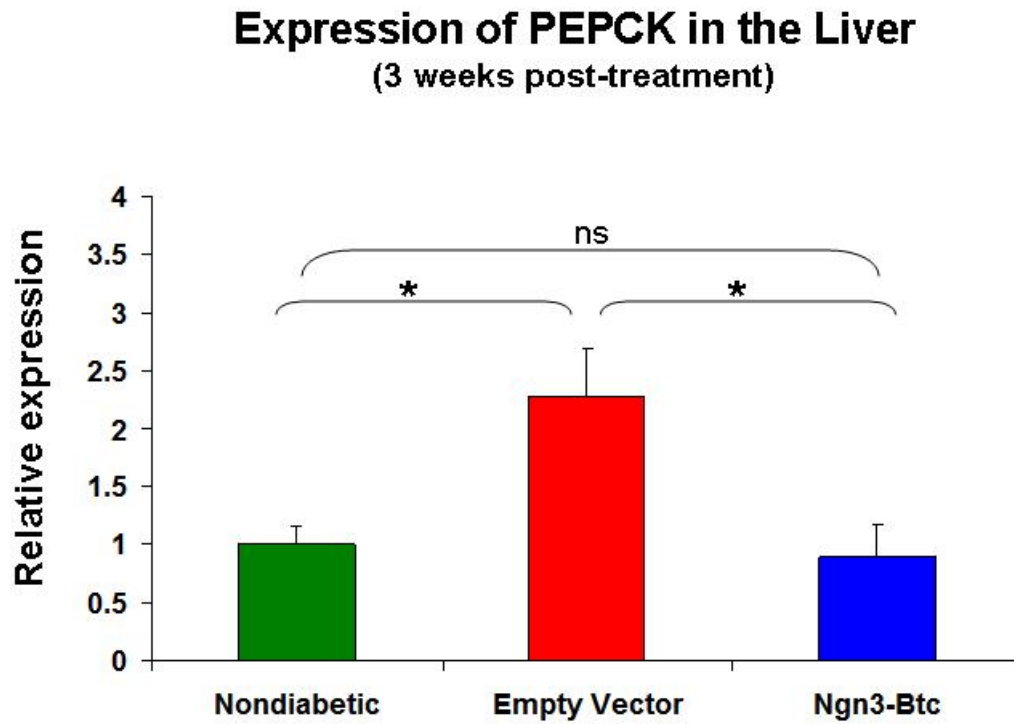
Supplemental Fig. 3



## Supplemental Fig. 4

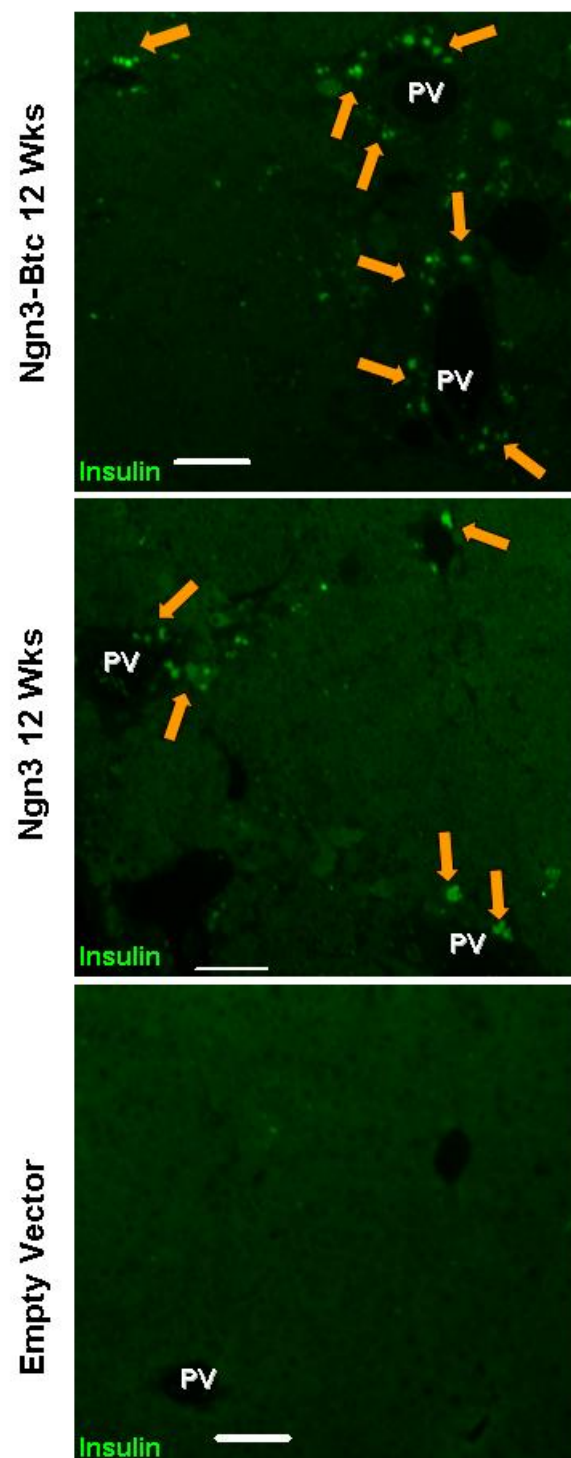


Supplemental Fig. 5



All values are in arbitrary units normalized to housekeeping gene expression

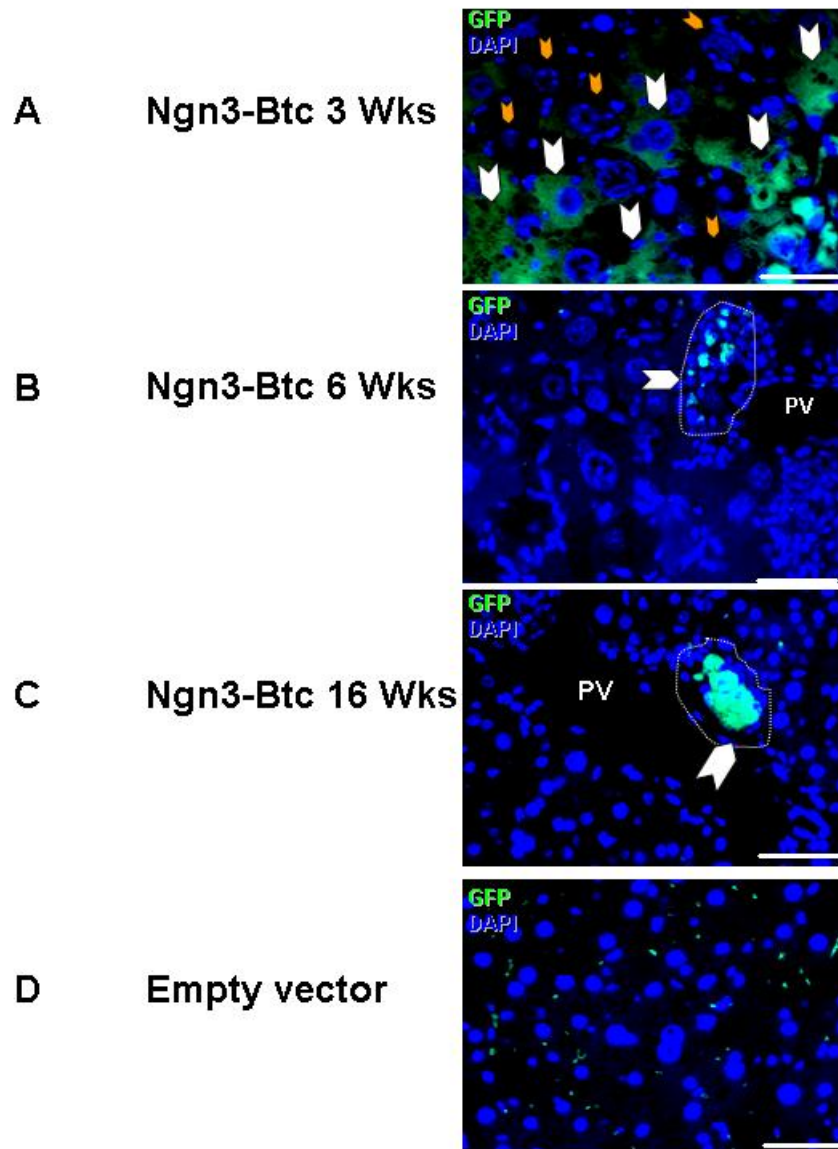
## Supplemental Fig. 6 Treated STZ-diabetic Liver





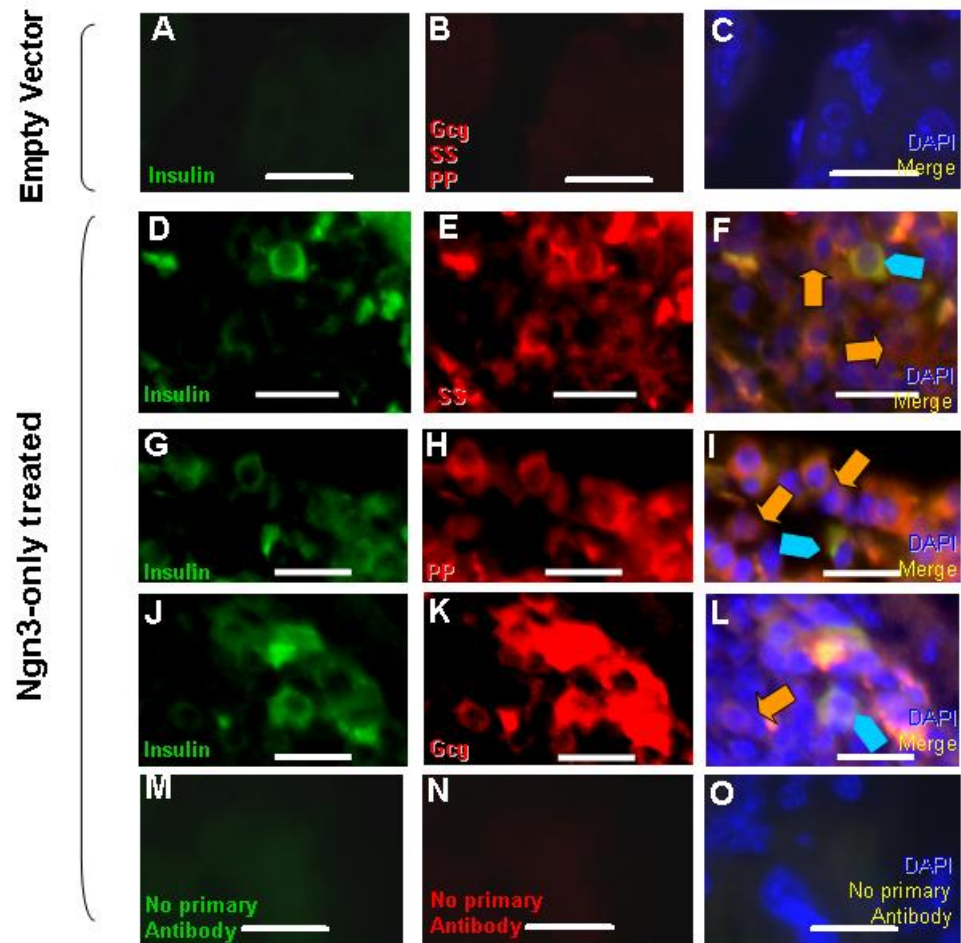
## Supplemental Fig. 7

## STZ-diabetic mip-GFP Tg Mice



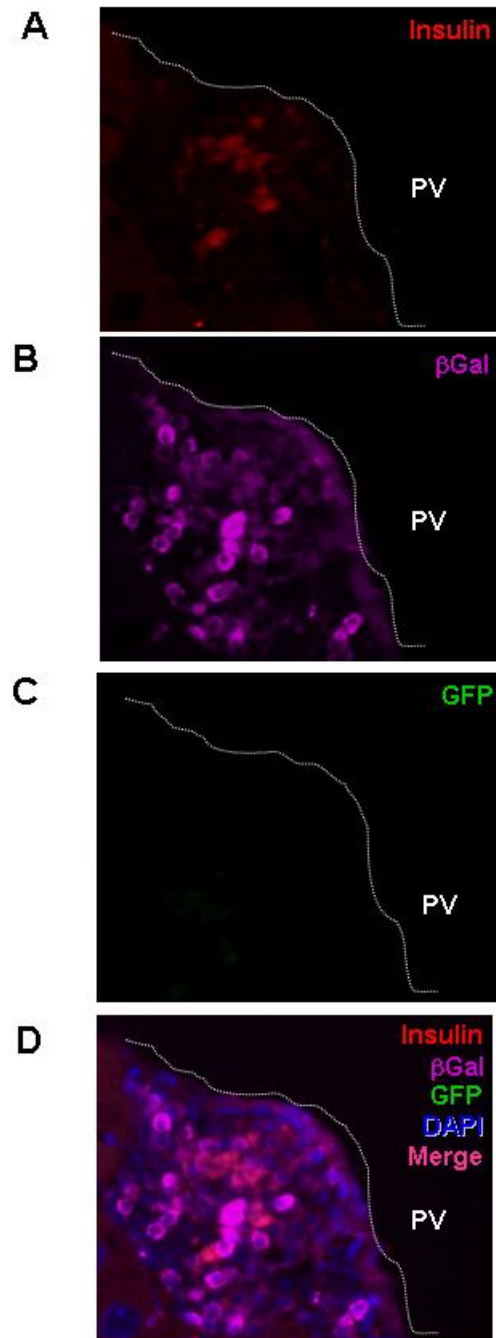
## Supplemental Fig. 8

## Islet Hormones in treated STZ-Diabetic Liver – 6 Wks

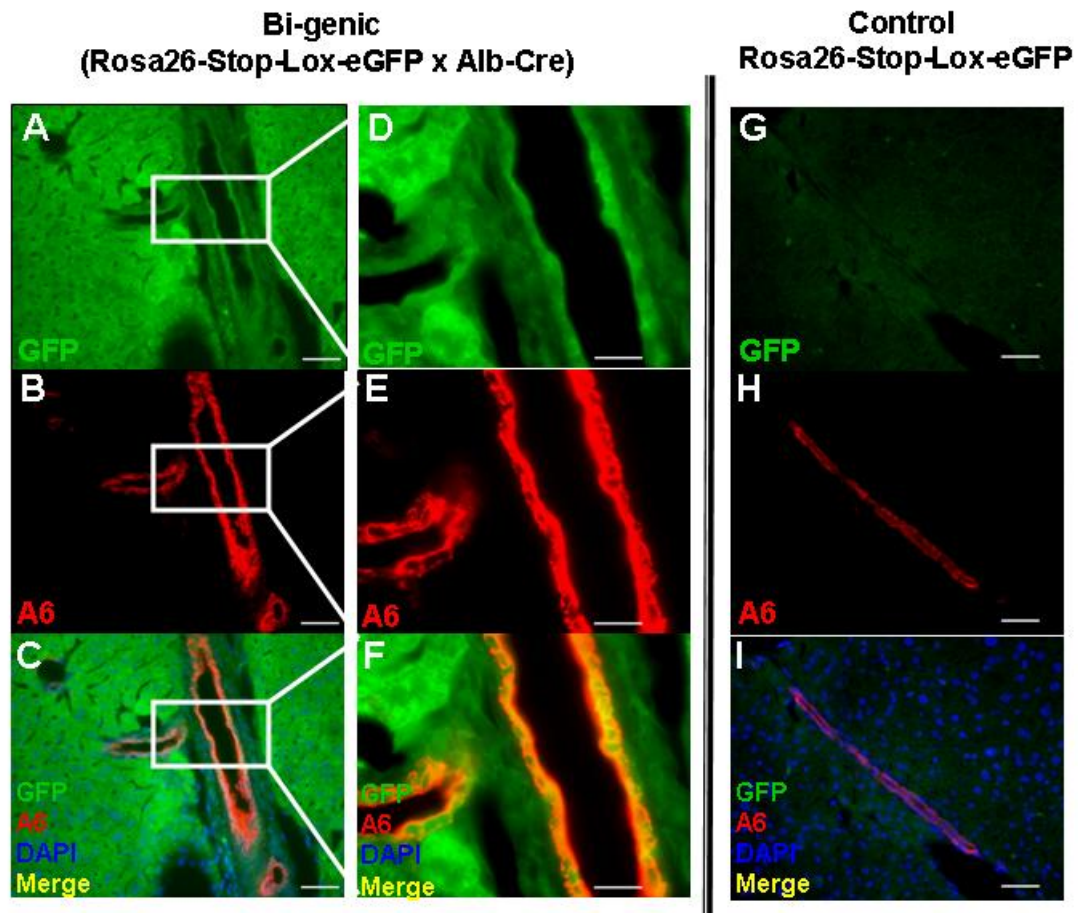


## Supplemental Fig. 9

Donor Bone marrow – mip-GFP transgenic mice  
Recipient – Rosa26-LacZ transgenic mice  
Ngn3-Btc treated STZ-Diabetic Liver – 6 Wks

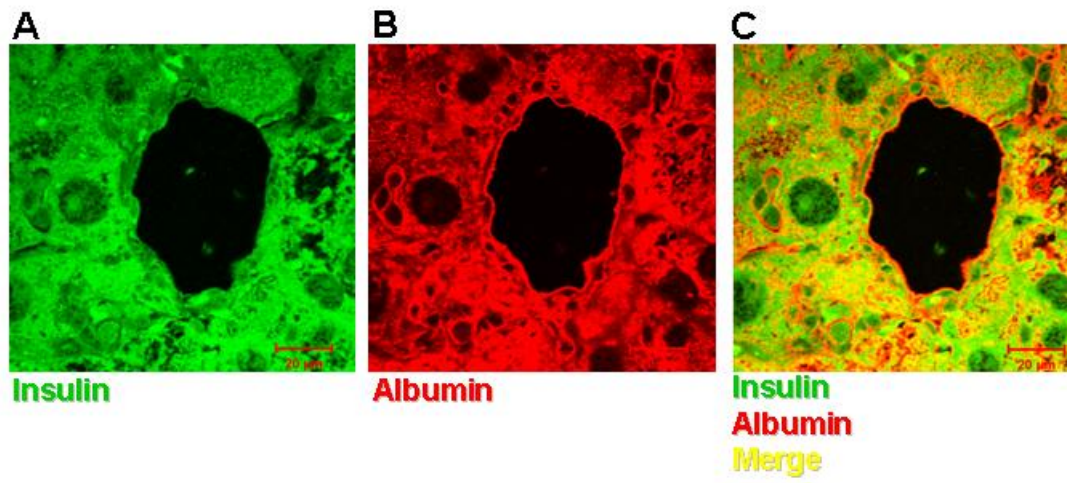


Supplemental Fig. 10



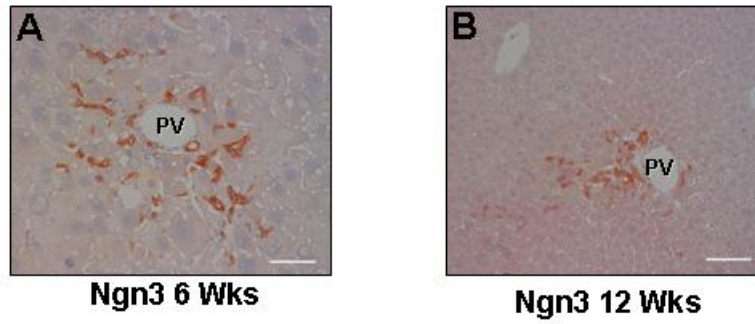
## Supplemental Fig. 11

## Ngn3-Btc treated STZ-Diabetic Liver – 3 Wks

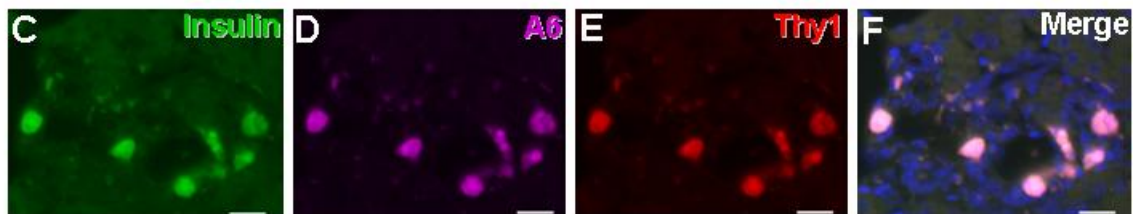


## Supplemental Fig. 12

## Ngn3-only treated STZ-Diabetic Liver A6 Immunostaining



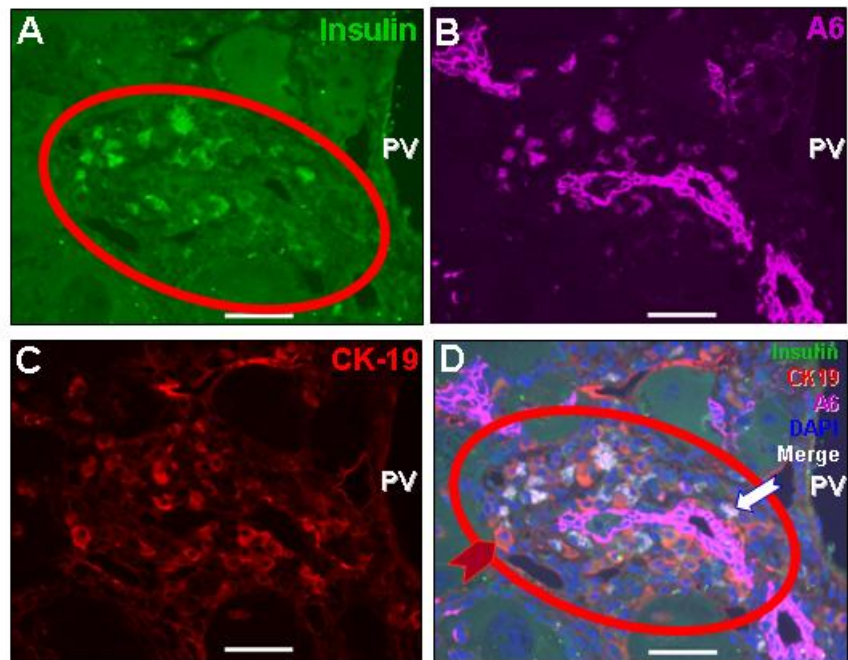
## Ngn3-Btc treated STZ-Diabetic Liver – 12 Wks





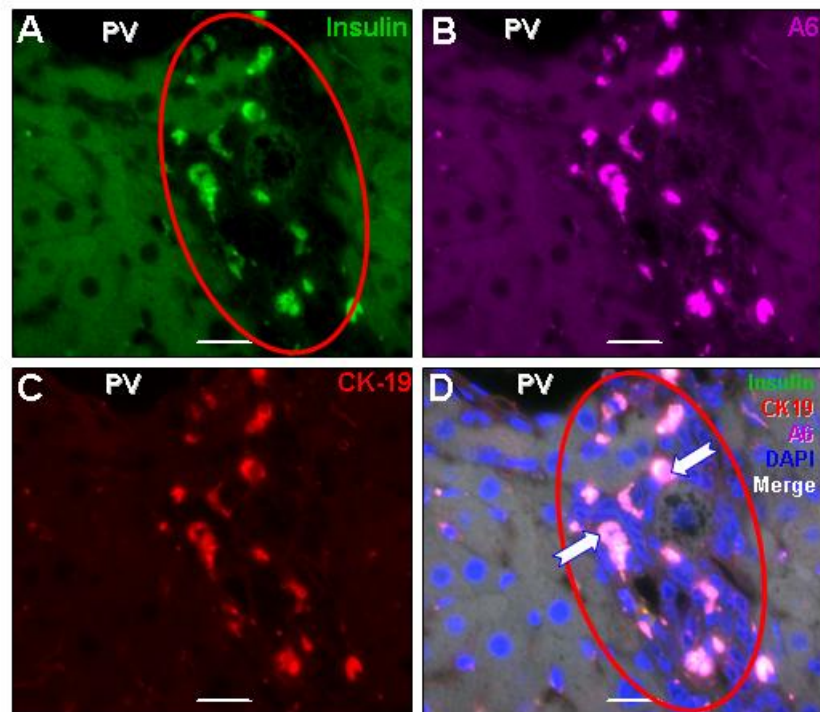
## Supplemental Fig. 13

## Ngn3-Btc treated STZ-Diabetic Liver – 12 Wks



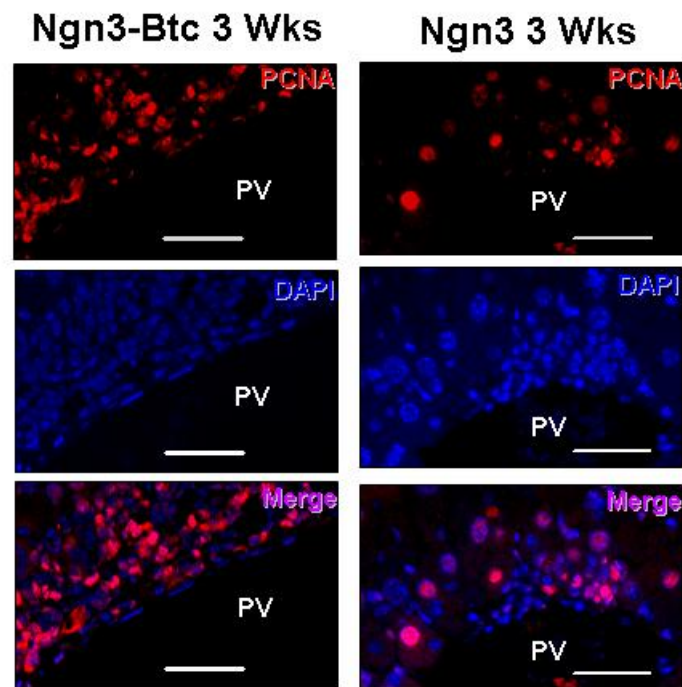
## Supplemental Fig. 14

## Ngn3-only treated STZ-Diabetic Liver – 12 Wks

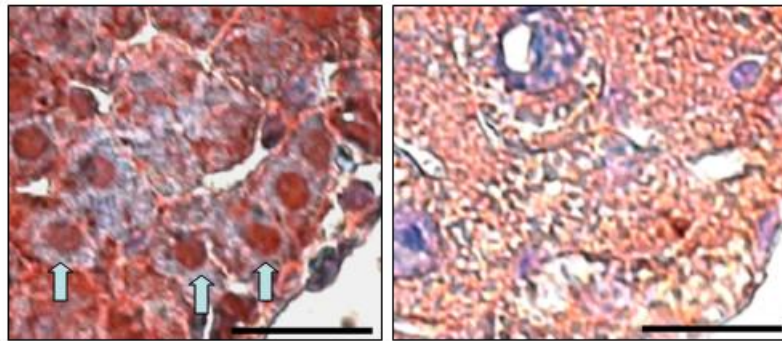


## Supplemental Fig. 15

## PCNA Staining



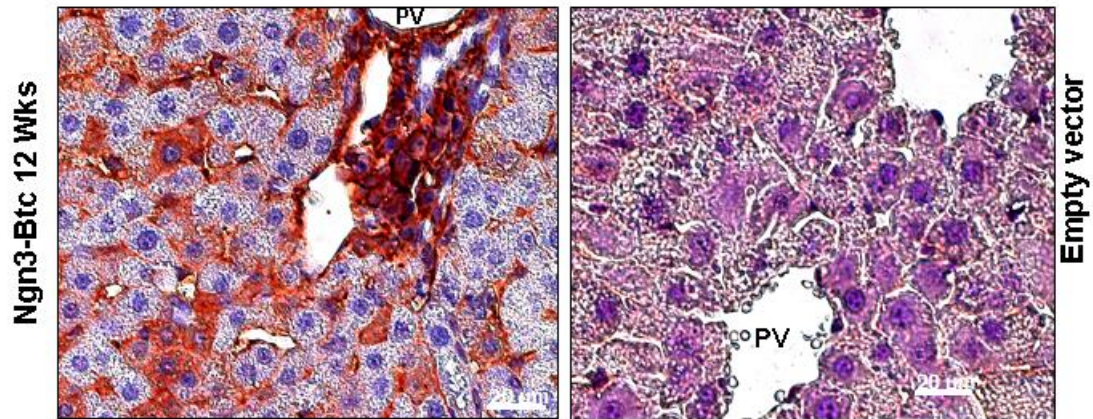
## Supplemental Fig. 16

**Pdx-1 Immunostaining****Ngn3-Btc****Empty Vector****Nuclear localization of immunoreactive Pdx-1 in the periportal cells in the Ngn3-Btc treated mice (arrows)**

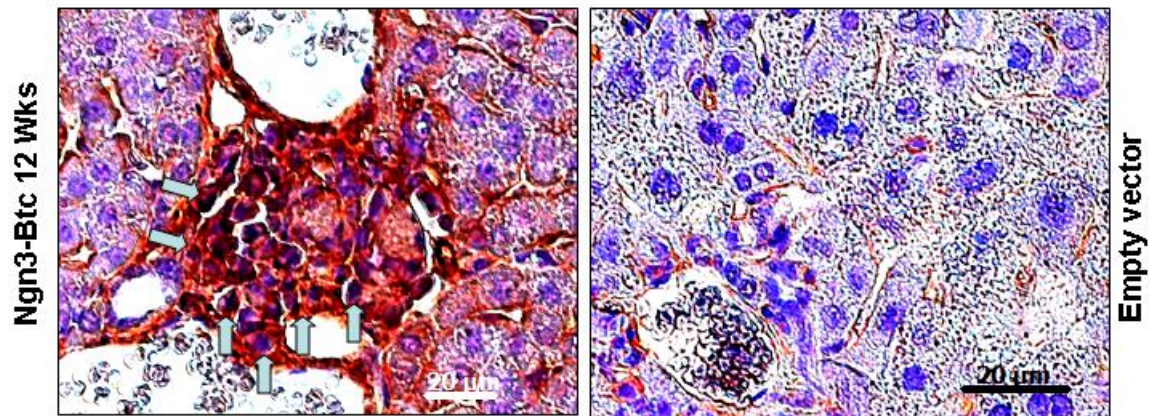


## Supplemental Fig. 17

## Ngn3 Immunostaining



## Nkx6.1 Immunostaining



Predominantly nuclear localization of immunoreactive Nkx6.1 in the periportal cells in the Ngn3-Btc treated mice (arrows)

## Supplemental Fig. 18

## Betacellulin Immunostaining

